1994-05-01

High Resolution Liquid Crystal Phase Grating Formed by Fringing Fields From Interdigitated Electrodes

Gregory P. Nordin
nordin@byu.edu

M. Friends

J. M. Jarem

S. T. Kowel

J. H. Kulick

See next page for additional authors

Original Publication Citation

R. G. Lindquist, J. H. Kulick, G. P. Nordin, J. M. Jarem, S. T. Kowel, M. Friends and T. Leslie,"High Resolution Liquid Crystal Phase Grating Formed by Fringing Fields From Interdigitated Electrodes" Opt. Lett. 19(9), pp. 67-72 (1994)

High-resolution liquid-crystal phase grating formed by fringing fields from interdigitated electrodes

R. G. Lindquist, J. H. Kulick, G. P. Nordin, J. M. Jarem, S. T. Kowel, and M. Friends

Department of Electrical and Computer Engineering, University of Alabama in Huntsville, Huntsville, Alabama 35899

T. M. Leslie

Department of Chemistry, Material Science Program, University of Alabama in Huntsville, Huntsville, Alabama 35899

Received November 18, 1993

We report the formation of thin anisotropic phase gratings in a nematic liquid-crystalline film by use of lateral (fringing) electric fields induced by transparent interdigitated electrodes. These gratings yield high diffraction efficiency (>30%) with a strong dependence on the readout beam incidence angle. In addition, the formation of a defect wall is observed that has a significant effect on the diffraction properties of the phase grating.

Electrically controlled phase gratings have potential applications in high-resolution displays, three-dimensional displays,[1] optical interconnections,[2] and diffractive optical elements. Such phase gratings should offer both high diffraction efficiency (>30%) and high spatial frequency (>1000 line pairs/mm). One method of realizing these properties is to utilize fringing electric fields from interdigitated electrodes penetrating a thin film of homeotropically aligned liquid-crystalline material. The deformation of the liquid crystal in the presence of the electric field creates an anisotropic phase grating with a period limited by only the lithographic process used to fabricate the interdigitated electrodes. For example, we have successfully fabricated such phase gratings with periods as small as 0.8 μm, which we believe to be the highest spatial frequency (1250 line pairs/mm) ever formed by electrodes in liquid-crystalline material.

In this Letter we discuss the diffractive properties of liquid-crystal anisotropic phase gratings and report a curious dependence of diffraction efficiency on the incident angle of the readout beam. Although the results discussed herein are based on experimental measurements of liquid-crystal gratings of a period of 8 μm, they are indicative of measurements performed on cells having periods between 2 and 16 μm. The primary issues addressed are (1) the significant effect of a defect wall on the diffraction efficiency at normal incidence and (2) an asymmetric energy transfer characteristic of blazed gratings observed at off-normal-incidence readout beam angles. The diffraction behavior is qualitatively explained by use of a simple model of the spatially varying liquid-crystal director axis.

Prost and Pershan[3] were the first to study diffraction from a phase grating created in a homeotropically aligned film of liquid crystal deformed by fringing fields caused by interdigitated electrodes. Their main objective was to investigate the flexoelectric effects of nematic and smectic-*A* liquid crystals by observation of diffraction from the periodic structure at twice the electrode pitch. Since their cells used opaque metal electrodes, diffraction from the fixed amplitude grating was mixed with the diffraction from the phase grating created by the quadratic electro-optic effect. Because our interest is in studying the diffraction resulting from this quadratic electro-optic effect, transparent indium tin oxide (ITO) electrodes were used to provide the fringing fields. We formed the electrodes, using conventional photolithographic and wet-etch techniques.

Figure 1 illustrates the formation of a phase grating in a thin film of homeotropically aligned liquid crystal with ITO interdigitated electrodes. As the figure shows, a spatially varying director-axis orientation is formed in the presence of an ac square wave applied to the electrodes. Ideally the liquid crystal will tend to align its director axis along the field lines. However, a splay-bend defect wall (sometimes referred to as a Helfrich wall[4]) and a line disclination form at the center between the electrodes, as a result of the director axis having to align itself from parallel ($+x$) to antiparallel ($-x$) with respect to the electric field lines. Modeling of the formation of the wall and the line disclination and their dynamic behavior would require the simultaneous solution of an inhomogeous anisotropic electrostatic system

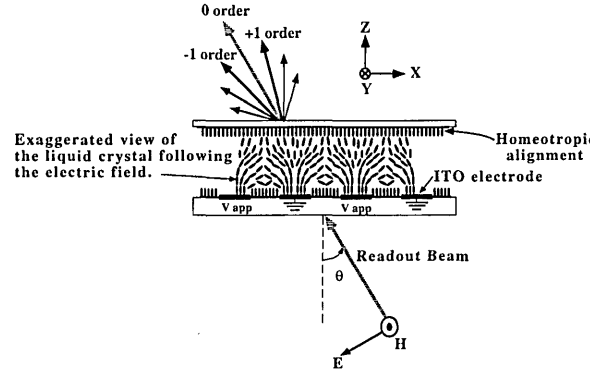

Fig. 1. Deformation of a homeotropically aligned liquid-crystal film by an electric fringing field from interdigitated electrodes.

0146-9592/94/090670-03$6.00/0

coupled with a nonlinear analysis of the elastic forces of the liquid-crystal molecules. Although some research has been done to address the numerical modeling of disclinations and defect walls in liquid crystals,[5] it is still in its initial stages and is beyond the scope of this Letter.

We can observe the defect wall by placing the liquid-crystal cell (a cross section of which is shown schematically in Fig. 1) between crossed polarizers in a polarizing microscope. Light that is transmitted through that portion of the sample in which there is zero phase retardation (a region that maintains homeotropic alignment) is extinguished by the exit polarizer, and such regions appear dark. Light from those portions of the sample that have a finite amount of the phase retardation (regions in which the liquid-crystal director axis deforms away from homeotropic alignment) is not extinguished by the exit polarizer, and such regions appear bright. Figure 2 shows a photomicrograph of a liquid-crystal grating structure in which a 200-Hz, 4-V square wave is applied to ITO interdigitated electrodes having a 4-μm finger width and an 8-μm pitch. The director-axis alignment directly above the electrodes maintains a homeotropic alignment and appears as a thick black line. The thin black line between pairs of electrodes is due to the defect wall. As the electrode voltage is increased, the width of the defect wall narrows. The defect wall remains stationary, as long as the frequency of the electrode voltage is greater than 100 Hz.

In our diffraction experiments light from a linearly polarized He–Ne laser was used to illuminate a liquid-crystal cell composed of a 4-μm-thick liquid-crystal layer. The homeotropically aligned Merck BL009 (Ref. 6; $\Delta n \approx 0.29$) was sandwiched between glass plates. ITO interdigitated electrodes (4-μm finger width, 8-μm pitch) had been fabricated on one of the glass plates; the other glass plate was not coated with ITO.

We investigated the dependence of the diffraction efficiencies for the first six orders as a function of electrode voltage and readout beam incidence angle. Figure 3 shows an example of the experimental results for the ± 1 and ± 2 orders at incidence angles of 0° and 30°. At normal incidence the diffraction efficiency of the same positive and negative orders are identical, with the unusual feature of a large energy transfer to the ± 2 orders. The maximum diffraction efficiency of the second order ($\approx$16%) is twice as large as that of the first order ($\approx$8%). This implies a periodic structure at one half the electrode pitch, which coincides with the observed defect wall.

As the angle of incidence is increased to 30°, two striking characteristics emerge. First, the diffraction efficiencies of the corresponding positive and negative orders differ. The maximum diffraction efficiencies for the negative orders ($\approx$30% for -1 and $\approx$16% for -2) are at least twice as large as those for positive orders ($\approx$15% for $+1$ and $\approx$7% for $+2$). This asymmetric energy transfer is characteristic of blazed phase gratings.[7] Second, the ± 2 orders, which were dominant at normal incidence, have a lower maximum diffraction efficiency than the ± 1 orders. At larger incident angles the defect wall appears to have a less-significant effect on diffraction efficiency. To explain the qualitative properties of the diffraction efficiency we begin by making some assumptions about the refractive-index profile created by the liquid-crystal deformation. First, we reduce the problem to a single layer of liquid-crystal molecules in which the periodically varying director axis is represented by an average tilt angle $\Psi(x)$ with respect to the z axis. Second, as with the deformation observed with microscopy, the average tilt angle is assumed to follow an elliptical curve, with the defect wall added at the center between two adjacent electrodes. An extraordinary ray (TM wave) incident upon the cell will see an effective refractive-index profile $n_{\text{eff}}(\theta, x)$ that can be calculated by solution of the transcendental equation involving the index ellipsoid[8] and Snell's law, given by

$$n_{\text{eff}}^2(\theta, x) = \frac{n_\perp^2 n_{||}^2}{n_\perp^2 \sin[\theta_{\text{LC}} + \Psi(x)] + n_{||}^2 \cos[\theta_{\text{LC}} + \Psi(x)]},$$

$$n_{\text{eff}}(\theta, x) = \frac{n_{\text{air}} \sin\theta}{\sin\theta_{\text{LC}}},$$

where θ is the incident readout beam angle, θ_{LC} is the propagation angle of the TM ray in the liquid crystal, and $n_\perp$ ($\approx$1.527) and $n_{||}$ ($\approx$1.818) are the principal indices of refraction. The refractive-index

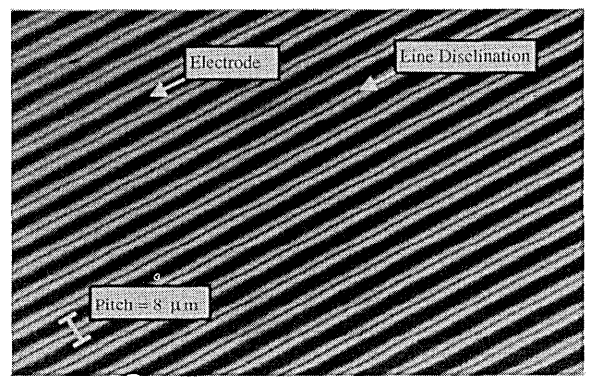

Fig. 2. Photomicrograph of the phase-grating structure between cross polarizers. The thick lines are electrodes and the thin lines are defect walls.

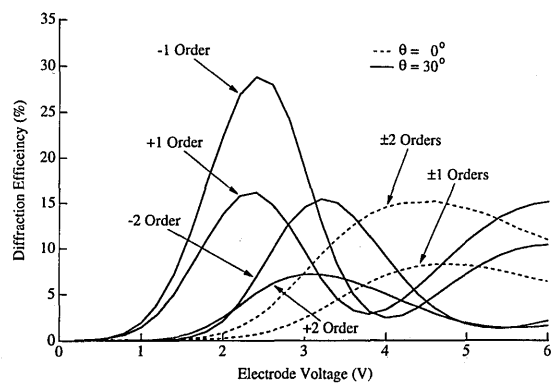

Fig. 3. Plot of experimental results for the diffraction efficiency of the ± 1 and ± 2 orders at incident angles of 0° and 30° as a function of electrode voltage.

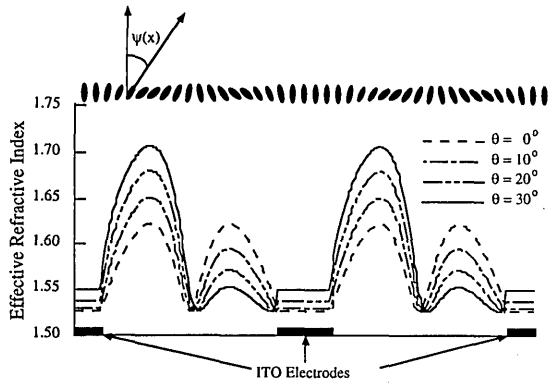

Fig. 4. Effective refractive-index profile for a TM wave at incident angles of 0°, 10°, 20°, and 30°.

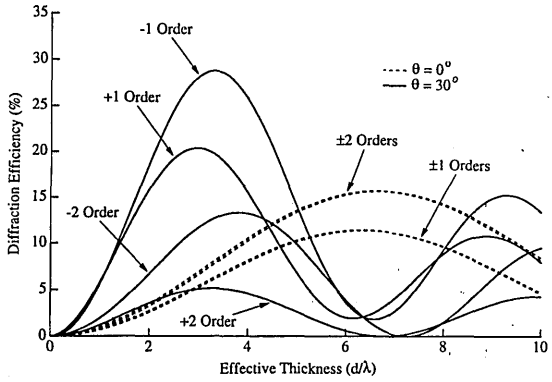

Fig. 5. Plot of numerical results for the diffraction efficiency of the ±1 and ±2 orders at incident angles of 0° and 30° as a function of effective film thickness.

profiles for incident angles of θ = 0°, 10°, 20°, and 30° are shown in Fig. 4. As the figure illustrates, the refractive-index profile is highly dependent on the incidence angle of the readout beam. At normal incidence the profile is symmetric, with a large dip at the center between adjacent electrodes. The symmetry of the profile is consistent with the observation of identical negative and positive orders. The large dip at the center caused by the defect wall provides the strong periodic structure at half the electrode pitch and results in a large energy transfer to the ±2 orders. As the incidence angle is increased, the profile becomes highly asymmetric. The maximum modulation depth is increased, and the modulation depth of the dip caused by the defect wall is less severe.

To test our assumptions about the liquid-crystal deformation we performed a thin phase-grating analysis on the refractive-index profile described in Fig. 4. We calculated the expected diffraction efficiency by determining the Fourier coefficients of the effective refractive-index profile. Numerical results for the diffraction efficiency of the ±1 and ±2 orders at 0° and 30° are shown in Fig. 5. In the numerical analysis the index profile remained fixed, as the effective thickness was increased. Increasing the thickness of the phase grating in the numerical analysis is comparable with increasing the voltage between interdigitated electrodes in the experiments because larger voltage implies increased penetration of the fringing electric field into the liquid-crystal film. In either case the strength of the grating is increased.

The same qualitative trends are observed in the numerical analysis as a function of thickness as are seen in the experiments as a function of voltage. At normal incidence the diffraction efficiencies of the corresponding positive and negative orders are identical, and a large energy transfer to the ±2 order is obtained. At an incident angle of 30° the asymmetric energy transfer is also reproduced, and the influence of the defect walls has diminished. Overall, the results from the thin phase-grating analysis qualitatively agree with the experimental results. Closer quantitative agreement would presumably require a more rigorous model of the liquid-crystal deformation.

In conclusion, liquid-crystal phase gratings based on fringing fields from ITO interdigitated electrodes display high diffraction efficiencies with a strong angle-of-incidence dependence. The highly anisotropic nature of the grating exhibits properties of blazed gratings, and these properties may make the grating useful for beam steering and diffractive applications. Currently research is being conducted to improve the modeling of the defect wall and line disclinations and to investigate the resolution limit of these liquid-crystal devices.

The authors gratefully acknowledge the support by the Advanced Research Projects Agency and the U.S. Army Missile Command under contracts DAH01-91-D-R005-D.O.18 and DAAH01-91-D-R-D.O.32.

References

1. J. Kulick, S. Kowel, T. Leslie, and R. Ciliax, Proc. Soc. Photo-Opt. Instrum. Eng. **1914,** 219 (1993).
2. M. Landgraf, C. Eldering, S. Kowel, and P. Brinkley, Proc. Soc. Photo-Opt. Instrum. Eng. **134,** 580 (1990).
3. J. Prost and P. S. Pershan, J. Appl. Phys. **47,** 2298 (1976).
4. S. Chandrasekhar, *Liquid Crystal,* 2nd ed. (Cambridge U. Press, New York, 1992), p. 135.
5. G. Haas, H. Wohler, M. W. Fritsch, and D. A. Mlynski, Mol. Cryst. Liq. Cryst. **198,** 15 (1991).
6. H. Dammann, Optik **31,** 95 (1970).
7. Commercially available from EM Industries, Inc., Hawthorne, N.Y. 10532.
8. A. Yariv, *Optical Electronics,* 4th ed. (Saunders, Philadelphia, Pa., 1991), p. 13–16.